JCTC Journal of Chemical Theory and Computation

Article

pubs.acs.org/JCTC

Modeling of Enhanced Catalysis in Multienzyme Nanostructures: Effect of Molecular Scaffolds, Spatial Organization, and Concentration

Christopher C. Roberts and Chia-en A. Chang*

Department of Chemistry, University of California, Riverside, California 92521, United States

ABSTRACT: Colocalized multistep enzymatic reaction pathways within biological catabolic and metabolic processes occur with high yield and specificity. Spatial organization on membranes or surfaces may be associated with increased efficiency of intermediate substrate transfer. Using a new Brownian dynamics package, GeomBD, we explored the geometric features of a surface-anchored enzyme system by parallel coarse-grained Brownian dynamics simulations of substrate diffusion over microsecond (μs) to millisecond (ms) time scales. We focused on a recently developed glucose oxidase (GOx), horseradish peroxidase (HRP), and DNA origami-scaffold enzyme system, where the H_2O_2 substrate of HRP is produced by GOx. The results revealed and explained a significant advantage in catalytic enhancement by optimizing interenzyme distance and orientation in the presence of the scaffold model. The planar scaffold colocalized the enzymes and provided a diffusive barrier that enhanced substrate transfer probability, becoming more relevant with increasing interenzyme distance. The results highlight the importance of protein geometry in the proper assessment of distance and orientation dependence on the probability of substrate transfer. They shed light on strategies for engineering multienzyme complexes and further investigation of enhanced catalytic efficiency for substrate diffusion between membrane-anchoring proteins.

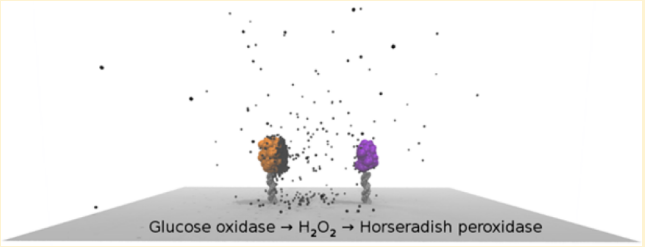

INTRODUCTION

Many biological catabolic and metabolic processes occur within colocalized multistep enzymatic reaction pathways with high yield and specificity.[1−5] In these complexes, the relative orientation and position of the enzymes can allow for efficient diffusion of substrates between the active sites of enzymes in the complex.[6,7] Enzymes often associate when freely diffusing in solution, but they also commonly associate on membrane surfaces, peripherally or as integral membrane proteins. The organization on surfaces has been proposed to increase local substrate concentration or substrate dwell time, caused by reduced dimensionality, potentially leading to additional gains in efficiency.[8−11] These factors may all help create an efficient environment for catalysis, but we do not fully understand their contribution to the efficiency of multienzyme constructs. A fundamental understanding of the factors that lead to this efficiency can result in engineered reaction-coupled enzyme systems in vitro to develop novel synthetic pathways or replace costly or wasteful existing procedures.

Techniques have been developed to create various types of spatially organized reaction-coupled enzyme systems.[4,12−19] Studies have explored fixating the relative positions of enzyme systems, such as anchoring enzymes to various molecular scaffold.[20−24] Recent advances in DNA synthetic procedures have been exploited for anchoring enzymes to various types of DNA scaffolds with highly accurate positioning.[20,25−30] Such experiments have attempted to establish the advantage of immobilizing enzyme systems and a relationship between enzyme distance and enhancement of enzyme efficiency.

Taking advantage of complementary nucleic acid base-pairing, Wilner et al. synthesized a flexible, hexagonal DNA scaffold with dangling DNA anchor points for two DNA-modified enzymes that share a product-reactant interdependence: glucose oxidase (GOx) and horseradish peroxidase (HRP).[20,31,32] The GOx-HRP system is an appropriate model for assessing the efficiency of spatially organized reaction-coupled enzyme systems because GOx produces H_2O_2 as a side product, a required cosubstrate for HRP turnover. The authors observed enhanced enzymatic efficiency because of enhanced interenzyme substrate transfer of H_2O_2 from GOx to HRP, showing the rate in the mutual turnover of GOx and HRP is dependent on this intermediate transfer under certain conditions.[20] Fu et al. expanded on this work by constructing a more rigid DNA origami surface with highly accurate programmable anchor points for the enzymes.[25] Enzymatic enhancement was high at small interenzyme distance, with reduced efficiency with increasing separation. The enhancement was considered due to increased local substrate concentration from restricted diffusion, attributable to the DNA scaffold. However, these conclusions remain controversial.[33]

Received: August 19, 2014
Published: December 2, 2014

dx.doi.org/10.1021/ct5007482 | J. Chem. Theory Comput. 2015, 11, 286−292

Previous work has used analytical approaches to characterize the efficacy of spatially organized systems under various conditions.[33,34] These insightful models account for important features of spatially organized systems over macroscopic time scales but are based on theory that may not fully consider the implications of subtle geometric features of scaffolded systems on the diffusive behavior of the substrate.[35,36] Previous computational simulations have shown promise in accurately describing diffusive behavior in the presence of coarse-grained (CG) biomolecular structures.[37−39] Bauler et al. used Brownian dynamics (BD) simulations to help characterize the effect of interenzyme distance and relative rotational orientation on intermediate substrate transfer in generic enzyme systems with simplified geometry.[38]

In this work, we explored the geometric features of an enzyme system anchored to a planar scaffold by using parallel CG BD simulations in microsecond to millisecond time scales. We investigated the mechanisms and revealed key features that enhance the efficiency of enzymes spatially organized on a DNA origami scaffold. We modeled the GOx-HRP system and assessed the substrate transfer probability dependence with spatial organization, system concentration, and surface scaffold interaction. We introduce BD simulation software, GeomBD, optimized for assessing specific geometric effects of large biomolecular systems over long time scales. To efficiently approach simulation over millisecond time scales, we developed this software by using modern parallelization techniques and a distance-dependent time-stepping algorithm.[40]

METHODS

We simulated a CG GOx-HRP scaffolded enzyme system using BD implemented in the GeomBD package. The H_2O_2 intermediate transfer, from the release site of GOx to the binding site of HRP, was simulated in parallel to determine the probability of binding-site association over the timespan of the turnover of the originating GOx enzyme (approximated as 300 s^{-1}).[25,41−43] Interenzyme distance, enzyme concentration, and the presence of scaffold were investigated for their impact on intermediate transfer.

Molecular Systems. The HRP isozyme C and GOx atomic structures were obtained from the protein data bank (PDB: 1ATJ and 1GPE, respectively).[44,45] CG enzyme models (Figure 1) were created from the obtained atomic PDB structures. Each amino acid was represented by an interaction sphere centered on the α-carbon of each residue. The radii of the amino acids were obtained from previous work: derived from hundreds of all-atom protein structures, the radii were calculated from the maximum distance from the α-carbon to all other atoms and then increased by a constant, 1.4 Å, to account for van der Waals radii.[46,47] Similarly, a CG H_2O_2 molecule was created by using a single bead with radius derived from the radius of gyration of the all-atom structure, then increased by the constant 1.4 Å, for a radius of approximately 2.5 Å. The DNA origami scaffold was represented by a simple 2D rectangular plane barrier of 60 by 80 nm, matching the dimensions of the experimental DNA tile.[25] The structural details of the DNA are abstracted into a smooth plane; thus, the results arising from this model are generalized to generic planar scaffolds. Explicit CG representations of the DNA strands that link each enzyme to the 2D scaffold were created from all-atom representations of a randomly sequenced DNA strand created using the NAB AMBER software interface.[48] For each nucleoside base in this CG DNA representation, two beads were positioned to represent the base and the associated sugar−phosphate backbone atoms. A Lennard-Jones-like potential was used for the CG ligand−protein and ligand−DNA linker interactions, as described previously, with the form

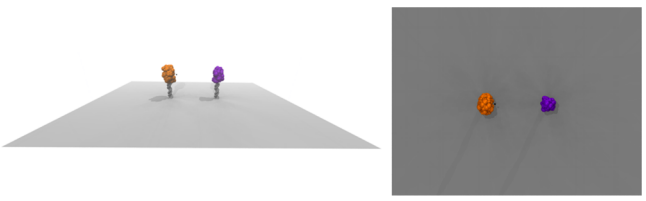

Figure 1. Coarse-grained model of glucose oxidase (GOx; left, orange) and horseradish peroxidase (HRP; right, purple) scaffold system. The 2D plane represents the DNA origami scaffold model, and a black sphere, close to GOx, represents the H_2O_2 substrate.

$$U = \frac{1}{2}\left(\left(\frac{\sigma}{r}\right)^8 - \frac{3}{2}\left(\frac{\sigma}{r}\right)^6\right)$$

where r is the distance between a ligand and an interaction bead, and σ is the sum of the radii of the two interacting spheres.[49] The ligand interaction with the 2D planar scaffold was modeled with the same potential, however, with the calculation of r modified for the implicit planar geometry. The radius of the implicit field radiating from the 2D planar scaffold was set to 1 nm to match the thickness of the experimental DNA origami tile.

The H_2O_2 CG model was assigned an experimentally determined diffusion coefficient of 1×10^{-3} nm^2/ps.[50] Electrostatic interactions between the ligand and other molecular structures were excluded from the simulations because of the neutrally charged substrate. Excluding electrostatic interactions isolates the effects brought about by the geometry of the spatially organized system without the system specific bias of long-range guided association. As shown previously, electrostatic interactions play a significant role in diffusive association in highly charged systems.[38] Thus, the impact of electrostatic interactions can be investigated in future studies using an embedded partial charge scheme. All structures, aside from the ligands, were held fixed in space during the simulations. Thus, no intramolecular potentials were included. A cubic simulation volume was used for all simulations. Volumetric bounds for all simulations involved periodic boundary conditions. As each simulation replicate contains one GOx enzyme, one HRP enzyme, and one substrate, the concentration of each solute was dictated by the simulation volume, with concentrations of 1, 10, and 100 nM corresponding to box edge lengths of approximately 1184, 550, and 255 nm, respectively (Figure 2).

Simulation Configuration. We performed a set of simulations over 1.5 μs at enzyme and substrate concentrations of 10 nM to assess the variance of interenzyme substrate transfer probability with spatial configuration. The simulations of GOx and HRP on a planar scaffold were performed at several interenzyme distances, measured from the anchor points: 10, 15, 20, and 25 nm. Because the enzyme orientations in situ cannot be fixed, simulation subsets were systematically performed with varying enzyme orientations. Starting from rotational states corresponding to the active sites of GOx and HRP directly facing each other, each enzyme was successively rotated 90° clockwise for a total of 16 combinations of GOx

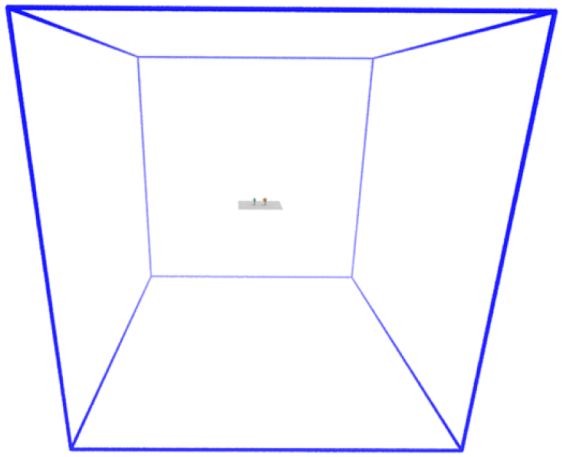

Figure 2. GOx-HRP-DNA origami-scaffold model centered in the cubic simulation volume corresponding to 100 nM system concentration. The box edge length is approximately 255.13 nm.

and HRP orientations (Figure 3). Thus, for each interenzyme distance, 16 simulation subsets were performed, each with 3000

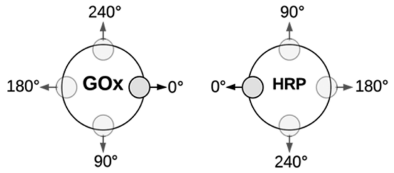

Figure 3. Top-down view of the rotational states for GOx and HRP varied in all subsets of simulation experiments. The gray circle represents the active site of each enzyme. Rotations were performed clockwise.

parallel replicates for a total of 48 000 parallel simulations for each interenzyme distance. Each 3000 replicate simulation was completed in approximately 3−5 h on 16 CPU cores.

To assess the role of the scaffold in the efficiency of initial ligand association probability, all simulations were repeated with the planar scaffold and DNA−linker molecules excluded while retaining the colocalized positions and orientations of the enzymes. This allowed for isolation of the effect of the scaffold beyond the effect of colocalization.

Long time scale (4 ms) simulations were performed to assess the efficacy of the scaffolded enzyme system relative to a solution of the substrate and an unmodified, unscaffolded target HRP enzyme. Because concentration effects are important at this time scale, simulations were performed with equal enzyme and substrate concentrations of 1, 10, and 100 nM.

Long time scale scaffolded simulations were performed with 16 orientation combinations in the same manner as described for the 1.5 us simulations. However, only a single interenzyme distance of 10 nm was simulated. Each enzyme orientation simulation set was replicated 3000 times, for 48 000 simulations per system concentration. Simulations were run in sets of 1000 replicates and completed in approximately 18 h running on 16 CPU cores.

A model of a disorganized solution containing an unmodified HRP enzyme with a freely diffusing H_2O_2 solute was simulated. For computational practicality, the CG HRP model was fixed in the center of the simulation volume. The substrate of each of 14 000 replicates was placed randomly in the simulation and allowed to diffuse either until associated with HRP or the 4 ms time limit was reached. These simulations were completed in batches of 2000 replicates, requiring 17−20 h running on 16 CPU cores.

Software Implementation and Optimization. GeomBD, our BD simulation software, was written in C++ with the CilkPlus extension for parallelization.[40] Because of the use of a generic short-range potential and omission of electrostatic interactions, the BD software is most appropriate for single-particle substrate diffusion investigations of the geometric effects of spatial configurations of large molecular systems. Though not used in the current work, electrostatic potentials are supported for single point charges centered in interaction spheres. To allow for electrostatic interaction of net neutral particles with a polarized charge distribution, rigid body partial charge embedding will be implemented for future investigation into system specific long-range electrostatic guidance and its effect on diffusional association.

The software was based on the first-order Ermak−McCammon equation for propagating the Brownian trajectory.[51−53] The BD algorithm was implemented with a distance-dependent time step ranging from 0.05 to 50 ps, depending on a ligand's distance, r, from the closest point to the enzyme−DNA system:

$$r < 10\ \text{nm}, \quad dt = 0.05\ \text{ps}$$
$$10\ \text{nm} < r < 25\ \text{nm}, \quad dt = 0.5\ \text{ps}$$
$$25\ \text{nm} < r < 50\ \text{nm}, \quad dt = 5.0\ \text{ps}$$
$$r > 50\ \text{nm}, \quad dt = 50.0\ \text{ps}$$

All parallel replicates independently advanced through time. The input file allows for configuration of all simulation parameters as well as manipulation of structure coordinates for ease of spatial configuration. Planar potential fields, such as that used for the DNA origami scaffold in this work, are added to a model system through the configuration file. Multiple planar potentials can be added for more complex arrangements. Although not used in the current work, cylindrical potential fields can be included in model systems for investigation of nanotube-like systems.

RESULTS AND DISCUSSION

Catalytic Enhancement on a Short Time scale. We performed a set of simulations over 1.5 μs to assess how differences in spatial configuration affect initial interenzyme substrate transfer probability of the GOx/HRP planar scaffold system. The model was sensitive to orientation and interenzyme distance and agreed with previously reported trends.[25,38] The highest probability of initial binding-site association occurred when the interenzyme distance was at its smallest value (10 nm) and the substrate release site of GOx directly faced HRP ($\theta_{GOx} = \theta_{HRP} = 0°$). Increasing the interenzyme distance affected the overall probability of substrate-binding-site association and induced an initial delay in the association distribution (Figure 4).

With rotation of the enzymes, the probability of substrate transfer decreased. However, because of the concave binding-site region of HRP, when only HRP was rotated 240 degrees, the binding site was partially oriented toward GOx, which led to behavior similar to unrotated HRP (Table 1). Analysis of the trajectories revealed that the general reduction in binding probability with rotation is due to the occlusion of the direct diffusion pathway from GOx to the binding site of HRP. The

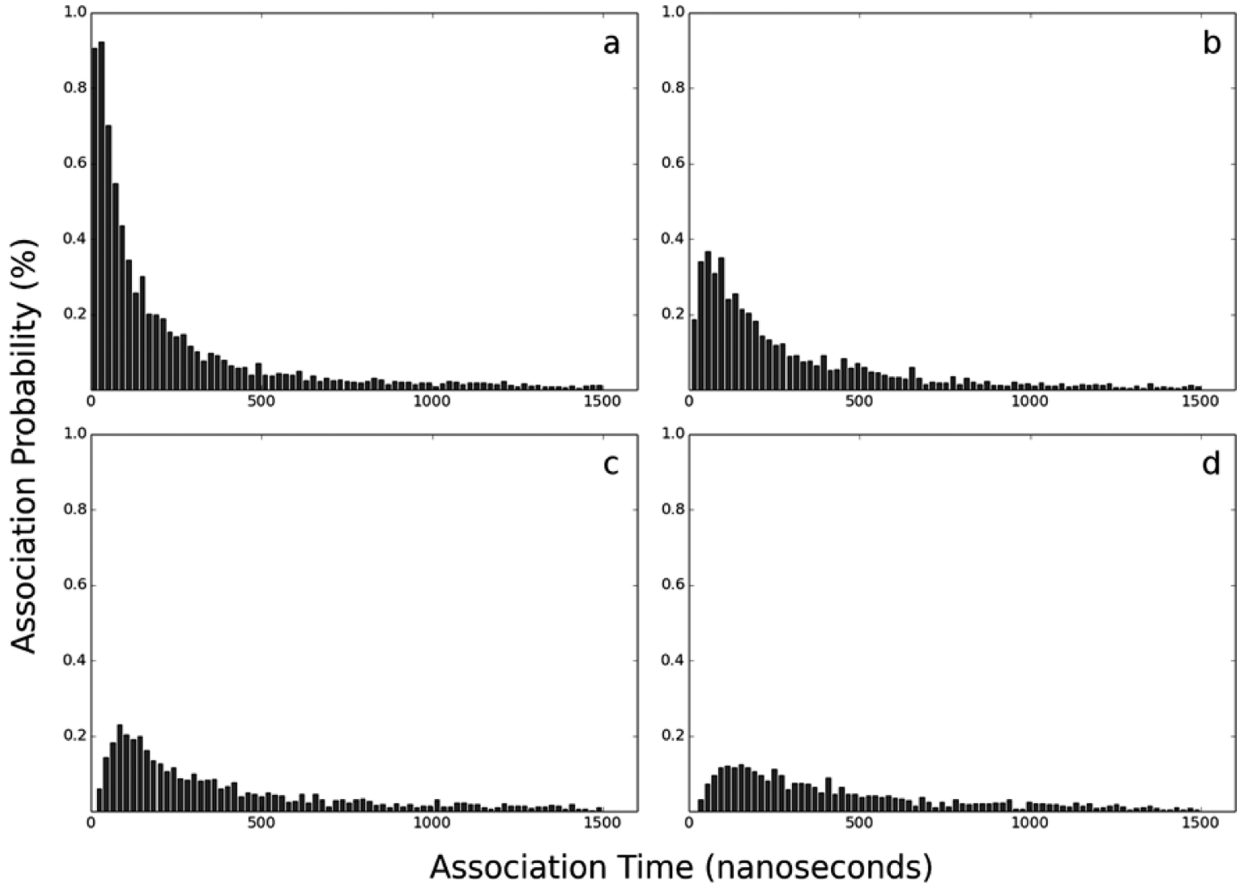

Figure 4. Binding time distribution for scaffolded GOx-HRP systems at different interenzyme distances. Each plot shows the percentage of ligands among 48 000 replicates (3000 × 16 orientational subsets) associated with the binding site of HRP within the first 1.5 μs with interenzyme distances of (a) 10 nm, (b) 15 nm, (c) 20 nm, and (d) 25 nm.

Table 1. Probabilities of Direct Stream Binding for Rotational Orientations of GOx and HRP Assembled on a Planar Scaffold at 10 nM Enzyme Concentration and 10 nm Interenzyme Distance

	$\theta_{GOx} = 0°$	$\theta_{GOx} = 90°$	$\theta_{GOx} = 180°$	$\theta_{GOx} = 240°$
$\theta_{HRP} = 0°$	0.127	0.083	0.060	0.070
$\theta_{HRP} = 90°$	0.090	0.068	0.055	0.051
$\theta_{HRP} = 180°$	0.085	0.059	0.043	0.057
$\theta_{HRP} = 240°$	0.117	0.088	0.055	0.067

Table 2. Fold Enhancement in Probability of Transfer for the Spatially Organized GOx-HRP Complex with and without a DNA Origami Scaffold[a]

interenzyme distance	colocalized complex with scaffold	colocalized complex without scaffold	fold enhancement due to scaffold
10 nm	0.073	0.055	1.34
15 nm	0.049	0.034	1.45
20 nm	0.038	0.023	1.65
25 nm	0.030	0.018	1.68

[a]Simulations were performed at various interenzyme distances, averaged across enzyme orientations, over 1.5 μs.

interenzyme distance and orientation dependence on efficiency are system-specific and suggest that the geometric details of the enzymes used for spatial organization study are important when modeling potential production systems.[38,54]

Role of Planar Scaffold on Initial Enhancement. The impact of the DNA origami-scaffold on initial binding after release of the substrate was determined by comparing simulations of the colocalized and spatially organized GOx-HRP system assembled on a planar scaffold with an artificially colocalized GOx-HRP model without a scaffold model. The results are significant for all interenzyme distances tested and are summarized in Table 2.

The overall transfer probability decreased with increasing interenzyme distance, but enhancement accountable to the scaffold increased with interenzyme distance. The planar scaffold blocked the diffusion of substrate in the direction of the scaffold. The substrate−scaffold affinity temporarily retained the substrate, allowing for transient 2D diffusion of the substrate on the plane. This led to longer substrate dwell times in the vicinity of the target enzyme relative to the artificially colocalized configuration. For most substrate, this retention was followed by diffusion back to the volume occupied by the enzymes. Approximately 18% of the total substrate from the planar scaffold simulation sets interacted with the scaffold. By the end of these simulations, 1% of the total substrate remained associated with the scaffold. This value is likely underestimated due to a lack of hydrodynamic interactions between the ligand and scaffold as well as a lack of atomic features on the planar scaffold. Regardless, this finding suggests that the scaffold has the potential to increase the local concentration of the substrate, in agreement with previous theoretical and experimental conclusions.[20,34]

dx.doi.org/10.1021/ct5007482 | J. Chem. Theory Comput. 2015, 11, 286−292

Catalytic Enhancement in Long Time scale. The efficiency of the planar scaffold model system over time on the order of the turnover of GOx was compared to that with a model of an unorganized solution of the substrate and target enzyme, HRP. Simulations were run for 4 ms simulation time to determine the cumulative probability of binding-site association of the substrate to HRP for the two systems. Because system concentration is relevant at this time scale, simulations were run at three system concentrations. Results are summarized in Table 3. In the most dilute solution (1 nM), the initial enhanced probability of substrate transfer with the scaffold system dominated the cumulative probability over the time period because of the relatively low rate of bulk substrate binding-site association in the unorganized solutions. The higher concentration solutions revealed nearly identical cumulative binding probabilities for the scaffolded and disorganized solution, with the binding distributions at the 100 nM concentration converging by 4 ms simulation time (Figure 5). Despite the convergence at higher concentration, the spike of initial binding probability within the first several microseconds after substrate release from GOx may still offer temporary kinetic advantages. Further optimization of initial interenzyme substrate transfer could result in improved kinetic advantages for spatially organized systems.

Table 3. Enhancement in Transfer Probability with the Spatially Organized Enzyme Complex System and Disorganized Solution of HRP and Substrate over Long Time Scales (4 ms)[a]

concn.	complex with scaffold	disorganized HRP-H_2O_2 solution	spatial organization fold enhancement
1 nM	0.10	0.02	5
10 nM	0.25	0.19	1.32
100 nM	0.89	0.87	1.02

[a]Cumulative binding-site association probabilities are compared at various system concentrations.

CONCLUSIONS

We used coarse grain Brownian dynamics simulations with the GeomBD package to assess enhancement in catalysis with spatial organization of GOx and HRP assembled on a planar scaffold. Our method builds on the findings of previous computational studies of interenzyme substrate transfer by including more system specific geometric detail and assessing the separate impacts of colocalization and assembly on a planar scaffold.

Colocalization of the enzymes dominated the enhancement of the planar scaffold-bound spatially organized system. Specifically, interenzyme distance and rotational orientation were the primary factors affecting the efficiency of our model enzyme system on a scaffold surface. The diffusive barrier induced by the scaffold played a significant but secondary role in the enhanced transfer. Maximum enhancement in intermediate transfer of the substrate was achieved for the enzyme system assembled on a planar scaffold with small interenzyme separation and enzyme binding sites oriented toward one another. Our results from varying enzyme orientation suggest that the geometric details of the enzymes used for spatial organization studies must be considered. As suggested, the interenzyme distance dependence on efficiency is also specific to the system geometry.[38,54]

With our model, a low system concentration is required to retain the initial benefit of spatial organization throughout millisecond time scales. At a higher concentration (100 nM), the cumulative probability of HRP−substrate association in the disorganized solutions competed with that the spatially organized system over 4 ms.

More complex spatial configurations that include compartmentalization of enzyme systems, which appear to offer

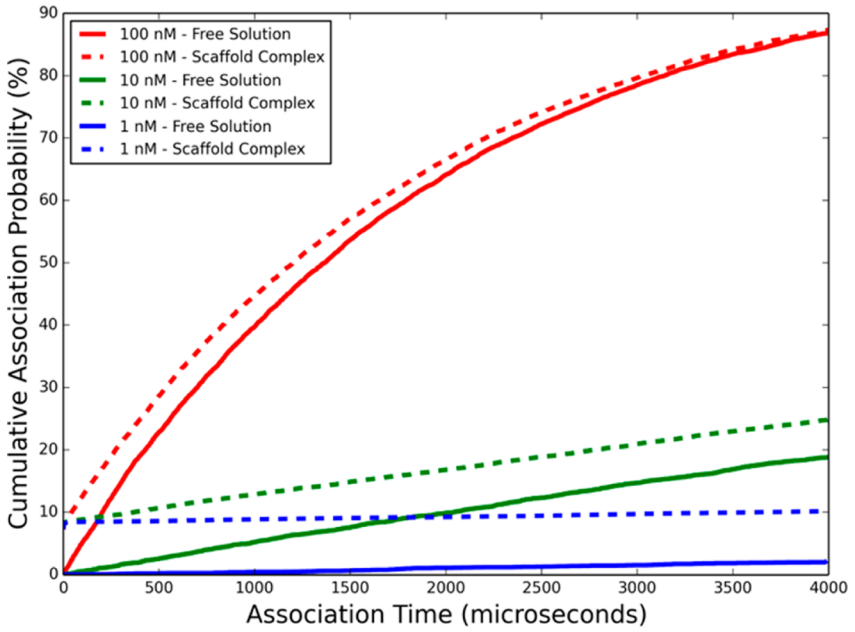

Figure 5. Probability of cumulative binding-site association comparison over 4 ms for spatially organized system and disorganized solutions at various system concentrations. For the scaffolded enzyme complex, the initial spike in binding-site association within the first microseconds of substrate diffusion after release from GOx may suggest a kinetic advantage of reaction-coupled enzyme systems assembled on a scaffold.

additional benefits to efficiency beyond that of a planar scaffold, will be explored computationally in the future.[55]

AUTHOR INFORMATION

Corresponding Author

*E-mail: chiaenc@ucr.edu. Phone: (951) 827-7263.

Author Contributions

The manuscript was written through contributions of all authors equally. All authors have given approval to the final version of the manuscript.

Funding

This work was supported by the U.S. National Science Foundation CAREER Grant MCB-1350401.

Notes

The authors declare no competing financial interest.

ACKNOWLEDGMENTS

We thank Dr. Ian Wheeldon at the University of California, Riverside for helpful discussions. Additional support from the University of California, Riverside, Computer and Communications, and XSEDE is gratefully acknowledged.

REFERENCES

(1) Kahn, R. A.; Fahrendorf, T.; Halkier, B. A.; Møller, B. L. Substrate Specificity of the Cytochrome P450 Enzymes CYP79A1 and CYP71E1 Involved in the Biosynthesis of the Cyanogenic Glucoside Dhurrin in Sorghum Bicolor (L.) Moench. *Arch. Biochem. Biophys.* **1999**, *363*, 9−18.

(2) Winkel, B. S. J. Metabolic Channeling in Plants. *Annu. Rev. Plant Biol.* **2004**, *55*, 85−107.

(3) Miles, E. W. The Molecular Basis of Substrate Channeling. *J. Biol. Chem.* **1999**, *274*, 12193−12196.

(4) Kim, Y. H.; Kwon, T. K.; Park, S.; Seo, H. S.; Cheong, J. J.; Kim, C. H.; Kim, J. K.; Lee, J. S.; Choi, Y. D. Trehalose Synthesis by Sequential Reactions of Recombinant Maltooligosyltrehalose Synthase and Maltooligosyltrehalose Trehalohydrolase from *Brevibacterium helvolum*. *Appl. Environ. Microbiol.* **2000**, *66*, 4620−4624.

(5) Jandt, U.; You, C.; Zhang, Y. H.-P.; Zeng, A.-P. Compartmentalization and Metabolic Channeling for Multienzymatic Biosynthesis: Practical Strategies and Modeling Approaches. *Adv. Biochem. Eng. Biotechnol.* **2013**, *137*, 41−65.

(6) Burack, W. R.; Shaw, A. S. Signal Transduction: Hanging on a Scaffold. *Curr. Opin. Cell Biol.* **2000**, *12*, 211−216.

(7) Savage, D. F.; Afonso, B.; Chen, A. H.; Silver, P. A. Spatially Ordered Dynamics of the Bacterial Carbon Fixation Machinery. *Science* **2010**, *327*, 1258−1261.

(8) Singer, S. J. The Molecular Organization of Membranes. *Annu. Rev. Biochem.* **1974**, *43*, 805−833.

(9) Adam, G.; Delbrück, M. Reduction of Dimensionality in Biological Diffusion Processes. In *Structural Chemistry and Molecular Biology*; Rich, A., Davidson, N., Eds.; W. H. Freeman and Co.: New York, 1968; pp 198−215.

(10) Axelrod, D.; Wang, M. D. Reduction-of-Dimensionality Kinetics at Reaction-Limited Cell Surface Receptors. *Biophys. J.* **1994**, *66*, 588−600.

(11) Hrazdina, G.; Jensen, R. A. Spatial Organization of Enzymes in Plant Metabolic Pathways. *Annu. Rev. Plant Physiol. Plant Mol. Biol. 43*, 241−267.

(12) Bülow, L.; Ljungcrantz, P.; Mosbach, K. Preparation of a Soluble Bifunctional Enzyme by Gene Fusion. *Bio/Technology* **1985**, *3*, 821−823.

(13) Conrado, R. J.; Varner, J. D.; DeLisa, M. P. Engineering the Spatial Organization of Metabolic Enzymes: Mimicking Nature's Synergy. *Curr. Opin. Biotechnol.* **2008**, *19*, 492−499.

(14) Ljungcrantz, P.; Carlsson, H.; Mansson, M. O.; Buckel, P.; Mosbach, K.; Buelow, L. Construction of an Artificial Bifunctional Enzyme, β-Galactosidase/Galactose Dehydrogenase, Exhibiting Efficient Galactose Channeling. *Biochemistry* **1989**, *28*, 8786−8792.

(15) Riedel, K.; Bronnenmeier, K. Intramolecular Synergism in an Engineered Exo-Endo-1,4-β-Glucanase Fusion Protein. *Mol. Microbiol.* **1998**, *28*, 767−775.

(16) Mao, Q.; Schunk, T.; Gerber, B.; Erni, B. A String of Enzymes, Purification, and Characterization of a Fusion Protein Comprising the Four Subunits of the Glucose Phosphotransferase System of *Escherichia coli*. *J. Biol. Chem.* **1995**, *270*, 18295−18300.

(17) De Pascale, D.; Di Lernia, I.; Sasso, M. P.; Furia, A.; De Rosa, M.; Rossi, M. A Novel Thermophilic Fusion Enzyme for Trehalose Production. *Extremophiles* **2002**, *6*, 463−468.

(18) Orita, I.; Sakamoto, N.; Kato, N.; Yurimoto, H.; Sakai, Y. Bifunctional Enzyme Fusion of 3-Hexulose-6-Phosphate Synthase and 6-Phospho-3-Hexuloisomerase. *Appl. Microbiol. Biotechnol.* **2007**, *76*, 439−445.

(19) Levasseur, A.; Navarro, D.; Punt, P. J.; Belaïch, J.-P.; Asther, M.; Record, E. Construction of Engineered Bifunctional Enzymes and Their Overproduction in *Aspergillus niger* for Improved Enzymatic Tools to Degrade Agricultural By-Products. *Appl. Environ. Microbiol.* **2005**, *71*, 8132−8140.

(20) Wilner, O. I.; Weizmann, Y.; Gill, R.; Lioubashevski, O.; Freeman, R.; Willner, I. Enzyme Cascades Activated on Topologically Programmed DNA Scaffolds. *Nat. Nanotechnol.* **2009**, *4*, 249−254.

(21) Delebecque, C. J.; Lindner, A. B.; Silver, P. A.; Aldaye, F. A. Organization of Intracellular Reactions with Rationally Designed RNA Assemblies. *Science* **2011**, *333*, 470−474.

(22) Dueber, J. E.; Wu, G. C.; Malmirchegini, G. R.; Moon, T. S.; Petzold, C. J.; Ullal, A. V.; Prather, K. L. J.; Keasling, J. D. Synthetic Protein Scaffolds Provide Modular Control over Metabolic Flux. *Nat. Biotechnol.* **2009**, *27*, 753−759.

(23) Mosbach, K.; Mattiasson, B. Matrix-Bound Enzymes. II. Studies on a Matrix-Bound Two-Enzyme-System. *Acta Chem. Scand.* **1970**, *24*, 2093−2100.

(24) Mingardon, F.; Chanal, A.; López-Contreras, A. M.; Dray, C.; Bayer, E. A.; Fierobe, H.-P. Incorporation of Fungal Cellulases in Bacterial Minicellulosomes Yields Viable, Synergistically Acting Cellulolytic Complexes. *Appl. Environ. Microbiol.* **2007**, *73*, 3822−3832.

(25) Fu, J.; Liu, M.; Liu, Y.; Woodbury, N. W.; Yan, H. Interenzyme Substrate Diffusion for an Enzyme Cascade Organized on Spatially Addressable DNA Nanostructures. *J. Am. Chem. Soc.* **2012**, *134*, 5516−5519.

(26) Rothemund, P. W. K. Folding DNA to Create Nanoscale Shapes and Patterns. *Nature* **2006**, *440*, 297−302.

(27) Seeman, N. C. Nanomaterials Based on DNA. *Annu. Rev. Biochem.* **2010**, *79*, 65−87.

(28) Lin, C.; Liu, Y.; Yan, H. Designer DNA Nanoarchitectures. *Biochemistry* **2009**, *48*, 1663−1674.

(29) Michelotti, N.; Johnson-Buck, A.; Manzo, A. J.; Walter, N. G. Beyond DNA Origami: The Unfolding Prospects of Nucleic Acid Nanotechnology. *Wiley Interdiscip. Rev. Nanomed. Nanobiotechnol. 4*, 139−152.

(30) Winfree, E.; Liu, F.; Wenzler, L. A.; Seeman, N. C. Design and Self-Assembly of Two-Dimensional DNA Crystals. *Nature* **1998**, *394*, 539−544.

(31) Veitch, N. C. Horseradish Peroxidase: A Modern View of a Classic Enzyme. *Phytochemistry* **2004**, *65*, 249−259.

(32) Raba, J.; Mottola, H. A. Glucose Oxidase as an Analytical Reagent. *Crit. Rev. Anal. Chem.* **1995**, *25*, 1−42.

(33) Idan, O.; Hess, H. Diffusive Transport Phenomena in Artificial Enzyme Cascades on Scaffolds. *Nat. Nanotechnol.* **2012**, *7*, 769−770.

(34) Idan, O.; Hess, H. Origins of Activity Enhancement in Enzyme Cascades on Scaffolds. *ACS Nano* **2013**, *7*, 8658−8665.

(35) Takahashi, K.; Arjunan, S. N. V.; Tomita, M. Space in Systems Biology of Signaling Pathways—Towards Intracellular Molecular Crowding In Silico. *FEBS Lett.* **2005**, *579*, 1783−1788.

(36) Ridgway, D.; Broderick, G.; Lopez-Campistrous, A.; Ru'aini, M.; Winter, P.; Hamilton, M.; Boulanger, P.; Kovalenko, A.; Ellison, M. J.

Coarse-Grained Molecular Simulation of Diffusion and Reaction Kinetics in a Crowded Virtual Cytoplasm. *Biophys. J.* **2008**, *94*, 3748−3759.
(37) Klann, M. T.; Lapin, A.; Reuss, M. Stochastic Simulation of Signal Transduction: Impact of the Cellular Architecture on Diffusion. *Biophys. J.* **2009**, *96*, 5122−5129.
(38) Bauler, P.; Huber, G.; Leyh, T.; McCammon, J. A. Channeling by Proximity: The Catalytic Advantages of Active Site Colocalization Using Brownian Dynamics. *J. Phys. Chem. Lett.* **2010**, *1*, 1332−1335.
(39) Klann, M.; Koeppl, H. Spatial Simulations in Systems Biology: From Molecules to Cells. *Int. J. Mol. Sci.* **2012**, *13*, 7798−7827.
(40) Blumofe, R. D.; Joerg, C. F.; Kuszmaul, B. C.; Leiserson, C. E.; Randall, K. H.; Zhou, Y. Cilk. *ACM SIGPLAN Not.* **1995**, *30*, 207−216.
(41) Frederick, K. R.; Tung, J.; Emerick, R. S.; Masiarz, F. R.; Chamberlain, S. H.; Vasavada, A.; Rosenberg, S.; Chakraborty, S.; Schopfer, L. M.; Schopter, L. M. Glucose Oxidase from *Aspergillus niger*. Cloning, Gene Sequence, Secretion from *Saccharomyces cerevisiae* and Kinetic Analysis of a Yeast-Derived Enzyme. *J. Biol. Chem.* **1990**, *265*, 3793−3802.
(42) Bright, H. J.; Gibson, Q. H. The Oxidation of 1-Deuterated Glucose by Glucose Oxidase. *J. Biol. Chem.* **1967**, *242*, 994−1003.
(43) Yamanaka, S. A.; Nishida, F.; Ellerby, L. M.; Nishida, C. R.; Dunn, B.; Valentine, J. S.; Zink, J. I. Enzymatic Activity of Glucose Oxidase Encapsulated in Transparent Glass by the Sol-Gel Method. *Chem. Mater.* **1992**, *4*, 495−497.
(44) Gajhede, M.; Schuller, D. J.; Henriksen, A.; Smith, A. T.; Poulos, T. L. Crystal Structure of Horseradish Peroxidase C at 2.15 A Resolution. *Nat. Struct. Biol.* **1997**, *4*, 1032−1038.
(45) Wohlfahrt, G.; Witt, S.; Hendle, J.; Schomburg, D.; Kalisz, H. M.; Hecht, H. J. 1.8 and 1.9 A Resolution Structures of the *Penicillium amagasakiense* and *Aspergillus niger* Glucose Oxidases as a Basis for Modelling Substrate Complexes. *Acta Crystallogr., Sect. D: Biol. Crystallogr.* **1999**, *55*, 969−977.
(46) Reva, B. A.; Finkelstein, A. V.; Sanner, M. F.; Olson, A. J. Residue-Residue Mean-Force Potentials for Protein Structure Recognition. *Protein Eng. Des. Sel.* **1997**, *10*, 865−876.
(47) Shen, T.; Wong, C. F.; McCammon, J. A. Atomistic Brownian Dynamics Simulation of Peptide Phosphorylation. *J. Am. Chem. Soc.* **2001**, *123*, 9107−9111.
(48) Pearlman, D. A.; Case, D. A.; Caldwell, J. W.; Ross, W. S.; Cheatham, T. E.; DeBolt, S.; Ferguson, D.; Seibel, G.; Kollman, P. AMBER, a Package of Computer Programs for Applying Molecular Mechanics, Normal Mode Analysis, Molecular Dynamics and Free Energy Calculations to Simulate the Structural and Energetic Properties of Molecules. *Comput. Phys. Commun.* **1995**, *91*, 1−41.
(49) Kang, M.; Roberts, C.; Cheng, Y.; Chang, C. A. Gating and Intermolecular Interactions in Ligand−Protein Association: Coarse-Grained Modeling of HIV-1 Protease. *J. Chem. Theory Comput.* **2011**, *7*, 3438−3446.
(50) Henzler, T. Transport and Metabolic Degradation of Hydrogen Peroxide in *Chara corallina*: Model Calculations and Measurements with the Pressure Probe Suggest Transport of H_2O_2 across Water Channels. *J. Exp. Bot.* **2000**, *51*, 2053−2066.
(51) Ermak, D. L.; McCammon, J. A. Brownian Dynamics with Hydrodynamic Interactions. *J. Chem. Phys.* **1978**, *69*, 1352.
(52) Długosz, M.; Zieliński, P.; Trylska, J. Brownian Dynamics Simulations on CPU and GPU with BD_BOX. *J. Comput. Chem.* **2011**, *32*, 2734−2744.
(53) Greives, N.; Zhou, H.-X. BDflex: A Method for Efficient Treatment of Molecular Flexibility in Calculating Protein−Ligand Binding Rate Constants from Brownian Dynamics Simulations. *J. Chem. Phys.* **2012**, *137*, 135105.
(54) Eun, C.; Kekenes-Huskey, P. M.; Metzger, V. T.; McCammon, J. A. A Model Study of Sequential Enzyme Reactions and Electrostatic Channeling. *J. Chem. Phys.* **2014**, *140*, 105101.
(55) Fu, Y.; Zeng, D.; Chao, J.; Jin, Y.; Zhang, Z.; Liu, H.; Li, D.; Ma, H.; Huang, Q.; Gothelf, K. V.; Fan, C. Single-Step Rapid Assembly of DNA Origami Nanostructures for Addressable Nanoscale Bioreactors. *J. Am. Chem. Soc.* **2013**, *135*, 696−702.